A Simplified Model of a Supercritical Power Plant* Technical Report

Wataro Shinohara† Daniel E. Koditschek‡

September, 1995

Abstract

We develop a simplified state-space model of a once-through supercritical boiler turbine power plant. This phenomenological model has been developed to facilitate analytical insight in support of our investigation of wide load cycling operations including startup and shut down. We compare our model to several more physically accurate (and far more complicated) models and provide as well some contrasting simulation results.

1 Introduction

Fossil fueled power plants convert chemical energy to electrical energy through the coordinated exchange of various intermediate forms of energy. [1] A number of distinct physical processes — fuel combustion in the furnace, heat

*This research has been supported by the Electric Power Research Institute under contract RP8030-17

†Visiting Research Fellow from Toshiba Corporation, Department of Electrical Engineering and Computer Science, University of Michigan, Ann Arbor, MI 48109-2110

‡Associate Professor, Department of Electrical Engineering and Computer Science, University of Michigan, Ann Arbor, MI 48109-2110

[1] We wish to acknowledge a number of invaluable conversations with Profs. R. Smoak, R. Lady, and C. Taft who have tremendously advanced our understanding of the physics underlying power generating plant operation.

transfer from flue gas to working fluid (water/steam) through the boiler wall, mechanical movement of turbine blades resulting from steam enthalpy drop — are all involved in the complete conversion cycle. The dynamic reponse of a power station is determined primarily by its "slowest" physics — heat exchange between the furnace and the working fluid. In this report we propose a simple model of heat exchange for a supercritical boiler turbine power station and compare it with a far more rigorously built simulator developed by EPRI [15] for operator training. Our goal is a simple, physically based dynamic model suitable for intelligent nonlinear controller design.

Various past legislative and economic constraints have imposed increasingly stringent requirements on plant operations necessitating increasingly reliable performance for ever wider operating ranges [1]. Retooling power plants to meet these requirements has been accompanied by the development of numerous research and engineering efforts to build rigorous models for boiler turbine operation over the last three decades. At the present time it seems fair to assert that most major utilities across the country have now or are scheduled shortly to have in place sophisticated digital controllers that can afford (almost arbitarily) complicated coordinated control of the various constituent processes involved in power generation. At the same time, there now exist sufficiently accurate physical models to permit exhaustive testing and analysis of the consequences of alternative control policies. Missing still, in our view, is a more phenomenological and higher level understanding of the large signal behavior of fossil fuel plants that might promote the design of more effective controllers that integrate various levels of operation in a predictable manner.

We focus exclusively on supercritical boilers wherein heat exchange takes place under pressures and temperatures well over the critical point of water. Under supercritical conditions, water changes uniformly into steam without boiling, promoting a "once-through" type steam generator configuration. It is generally acknowledged that the supercritical once through boiler offers increased efficiency [3] and presents greater opportunities for an "agile" response to changing load demand. By the same token, its behavior near the critical range is rather complicated and characterised by strongly nonlinear dynamics.

In this report, we present the first in a series of working papers that will develop a scalable yet tractable family of models suitable for controller design. The introduction concludes with a brief review of the relevant literature and a summary of the salient features of this initial modelling effort. Next, in Section 2, we present the model. The results of a simulation study that compares this model to the EPRI simulator are summarized in Section 3. Details of the physical derivations and a more extended discussion

of the limitations in our model are provided in the appendix.

1.1 Background Literature

1.1.1 Simulation Models and Linearized Approximations

The vast literature of existing approaches to fossil fuel power plant modeling seems to divide for the most part into two distinct categories. On one hand, there is a great amount of work stressing physical accuracy with the goal of developing numerical simulations — for example, static and dynamic finite element methods [2] — as a representation of the complex constituent physical phenomena that characterize the energy conversion process. Such simulation models are extremely valuable, and we will rely on one in particular, the EPRI sponsored operators' training package [15], mentioned above, to validate our own work. But these complex numerical models cannot be used to gain insight into the nature of the plant dynamics such as would be required for intelligent controller design.

In contrast, the prevailing industrial controllers typically consist of numerous PID loops [2, 9, 15] tuned in a more or less centralized manner to reflect plant engineers' intuition regarding the right settings for different operating regimes. With the advent of centralized digital sensing and computational systems, modern techniques of linear control theory have been introduced into an increasing number of operating plants as well [20]. In support of this industrial practice, a second major component in the power plant literature concerns the development of linear models [16, 17] designed around the plants' small signal behavior.

No doubt, at a specified operating point, properly tuned linear models provide the basis for developing excellent controllers [17]. Yet with the advent of industry deregulation, the need for safe and efficient adaptation to highly varying demand cycles, for fast response to unanticipated demand variations and for automated emergency response all present a compelling argument for a large signal (and, thus, nonlinear) design oriented plant model. This is the nature of the phenomenological model we have sought in the literature and begin to develop in this report.

1.1.2 Prior "Phenomenological" Models

Our development of a tractable large signal model with sufficient accuracy for controller design is based on previous work of a very few authors whose interest in phenomenological models — i.e., characterized by roughly accurate physics yet tractable mathematical structure — distinguishes them

in our view from the two distinct preponderant traditions of the literature remarked upon above. Initial work by Adams et.al. [5], although concerned with merely a linear approximation to the physical processes at hand , provides an analytical framework that forms the foundation for the subsequent "phenomenological" literature by deriving a lumped compartmental model that respects the conservation of energy, momentum, and mass. Ray [6] extended these ideas to develop a nonlinear compartmental model. Masada et.al. [8, 9] pursued a systematic investigation of lumped models for heat exchange and proposed criteria for determining the proper number of compartments. In all these papers, for each compartment, dynamics are developed according to physical conservation principles — a feature that we attempt to mimic in our even simpler version of the phenomena. In contrast to the work of Adams et al. [5], and Ray [6], which concerned subcritical plants, the work of Masada [7, 9] is particularly interesting to us in that it treats the supercritical boiler.

These prior "phenomenological" efforts are sufficiently concerned with physical accuracy to end up with numerous (in the tens) compartments, characterized by several (four or five) state variables. In contrast, we are primarily interested in understanding the overarching structure of the boiler response — the dominant dynamics in a generating plant. Thus, we use the previous literature to develop in this report a model with the minimal possible number of compartments (two) and states (one, and two) with the attitude that the resulting "cartoon" should offer significant insight into the large signal response of the power generating plant. If the "cartoon" is sufficiently faithful, then the structural features we identify will readily scale with the number of compartments and resolution of compartment model. [2]

1.2 Assessment of Present Results

Our model has been developed for general use, but it was tuned in this report so as to reproduce as closely as possible the operational response of a far more complex EPRI simulator [15], whose effective maximum generated power is taken to be 650MW (the nominal value is $750MW$). All the unknown parameters in our model were calibrated offline to operational data produced by the EPRI simulator, as described in Appendix Section 5.4.

The calibrated model predicts reasonably the generated power response of the EPRI simulator in the range of 65% to 90% load demand.

Not too surprisingly, the internal state(temperature, density etc.) re-

[2]The only other contribution we have found in the power generation literature that takes our point of view is the work by Åström et al. [4] where only one state for drum pressure is used for describing a drum boiler-turbine system.

sponse of our model fails to follow the corresponding state behaviors of the EPRI simulator. We attribute this internal discrepancy to the overly simplistic compartment boundary conditions consequent upon the absence of so many physical effects such as economizer input enthalpy etc. Further scaled up versions of this model will replace these artificially constant boundary conditions with functions of the added compartment states.

2 The Model

As explained above, we are most centrally interested in the mechanism of heat transfer from combustion to steam generation — the dominant dynamical feature of the power generation process. We consider a fixed length of "piping" in a typical once-through boiler, and focus on the transfer of heat from flue gas through the metal boiler wall to the working fluid. Abbreviating the phenomenological literature discussed above [5, 6, 9], we summarize the complicated physics as a two compartment lumped parameter system consisting of a "furnace," where burning fuel radiates heat energy through the wall to the working fluid, and a "superheater" where hot flue gases arising from the furnace section transfer heat energy through the wall by convection. [3]

Fig. 1 presents a simple block diagram of our plant model labelled with the principal variable names. In this formulation, water flow rate from economizer, w_{fw}, throttle valve opening, u_v, and heat transfer from wall, Q_{wf}, Q_{ws} (both assumed to be proportional to combustion heat Q_c , as described in Section 5.1.2), are regarded as control inputs, and generated power, W, is the output. Highly compressed water from the economizer, w_{fw}, flows through the furnace and the superheater receiving heat transferred from the wall in each section, Q_{wf}, Q_{ws}, and changes to steam all in a supercritical state (i.e., without any two phase phenomena). Superheated supercritical steam is directed into the turbine via throttle valve(s) which control steam flow rate, w_{fs}. The latter is directly proportional to the power generated by the turbine, W.

[3] The knowledgeable reader may further note that in our simplification of the development of Adams and Masada [5, 9] we have found it convenient to depart from their example by using temperature (and density in the furnace) as our state variable(s), rather than a more general form of internal energy. Aside from the slightly greater intuitive appeal, working with such directly measureable physical quantities has significantly facilitated our efforts to calibrate this model to the EPRI simulator (and thus, hopefully, someday, to a "real" plant).

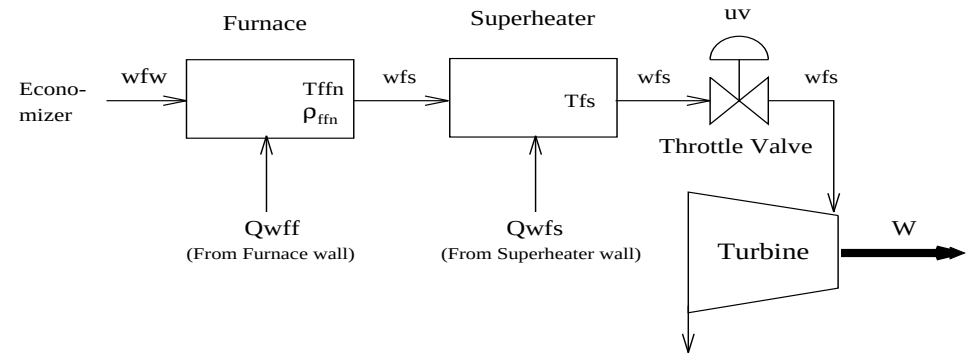

Figure 1: Simplified block diagram of a boiler-turbine power plant

2.1 Assumptions

In order to arrive at the plant depicted in Fig. 1, we first adopt many of the assumptions originally introduced in [5],

- working fluid properties are uniform at any cross section
- gas, wall, and fluid, heat conduction in the axial direction is negligible
- gas-pressure dynamics are negligible
- balanced flow and uniform heat flux prevail at any cross section in multitube heat-exchange boiler sections

In the interest of still greater simplicity, we depart from the earlier work by further assuming

- there are only two sections in the working fluid path — the furnace and the superheater
- each boundary of a section is fixed
- work by a set of the turbines, that is, high/intermediate/low pressure turbines, is represented as the work of a single turbine unit.
- due to the turbine assumption, the effect of the reheater section is taken into account in the superheater section
- the working fluid displays constant mass flow rate in the superheater but variable mass flow rate through the furnace section

The first and second of these new assumptions may be easily relaxed to scale our model back up to the previous literature. It remains to be seen whether the loss of the section boundary as a state variable will significantly change the structural properties of our model, and the re-introduction of a moving section would be one of the first tests we would be likely to impose in scaling back up to the previous literature.

As for the turbines, each turbine works almost identically from the viewpoint of the "enthalpy drop" through the unit, and their coordinated effect seems plausibly represented by a single turbine's. This assumption forces us to treat the superheater and the reheater as a single compartment. These assumptions could also easily be relaxed, if the model were scaled up, and the turbines and the reheater evaluated separately.

The last assumption lumps all the compressibility of the working fluid into the furnace section, yoking the density of the working fluid on either side of this compartment to the more directly controlled flow rates. [4].

A final set of assumptions justify the substitution of algebraic (steady state) models in place of the flue gas and wall dynamics as derived in the appendix, and further simplify the computation of heat transfer from gas to fluid.

- the gas and wall heat transfer dynamics are sufficiently rapid relative to the working fluid as to be negligible; we use a steady-state model as in the gas sections
- the flue gas displays ideal gas behavior with respect to pressure and mass flow rate
- Heat transfer from flue gas to wall is proportional to the combustion heat generated in the furnace[5]

2.2 Notation

The principal symbols for variables and parameters used in our model representations are as follows (the complete list is provided in the appendix).

[4]Masada [9] considered the compressibility effect in economizer and reheater sections

[5]This assumes the heat transfer gains of heat transfer are constant through an operational regime of interest. To the contrary, these gains are, of course, funcions of the plant states. In future work, we anticipate adding adaptive loops to compensate for their slowly but dramatically changing gains over large transient operations including startup and shut down.

States

Symbol	Phenomenon	Units
ρ_f	Density of steam in furnace section	lb/ft^3
T_f	Temperature of steam in furnace section	F
T_s	Temperature of steam in superheater section	F

Control inputs

Symbol	Phenomenon	Units
w_{fw}	Input water mass flow rate from economizer section	lb/h
$\frac{dM_c}{dt}$	Combustion rate of coal fuel	lb/h
u_v	Throttle valve opening($0 \leq u_v \leq 1$)	

Output

Symbol	Phenomenon	Units
W	Generated power	MW

Functions

Symbol	Phenomenon	Units	Definition
w_{fs}	Steam mass flow rate	lb/h	eq.(52), p.30
Q_c	Combustion Heat flow in furnace section 1	Btu/h	eq.(21), p.26
P_f	Pressure of steam in furnace section	psi	eq.(10), p.10
P_s	Pressure of steam in superheater section	psi	eq.(5), p.9
h_f	Steam enthalpy in furnace section	Btu/lb	eq.(11), p.10
h_s	Steam enthalpy in superheater section	Btu/lb	eq.(3), p.9

Constants

Symbol	Phenomenon	Units
ρ_s	Density of steam in super heater section	lb/ft^3
h_{fec}	Steam enthalpy in economizer section	Btu/lb
h_{cd}	Steam enthalpy in condensor section	Btu/lb

2.3 The Model

We summarize now the features of our model whose detailed derivation is presented in the Appendix, Section 5, using the assumptions listed above to greatly simplify the models introduced by Ray and Masada [6, 7, 9]. The

plant takes the form of a three state, three input, and one output dynamical system, that roughly represents the following physical effects.

2.3.1 The Output Map

Proceeding "backward" from the electric power output signal, when steam flows into the turbine an enthalpy drop from the super heater compartment, h_s, to the condenser, h_{cd}, causes work to be done on the turbine,

$$w_{fs}(h_s - h_{cd}) = K_{tb}W, \tag{1}$$

yielding the output variable, power, W of Figure 1. As elaborated in Appendix 5.2.1, the flow rate of superheated steam, w_{fs}, is directly adjusted by the throttle valve, u_v,

$$w_{fs} = \frac{k_v P_s}{\sqrt{T_s}} u_v. \tag{2}$$

which we take to be a control input.

The enthalpy in the condenser, h_{cd}, we take to be a constant. In contrast, the enthalpy in the superheater, h_s, we obtain via the state equation

$$h_s = h_{sc}[P_s, T_s] \tag{3}$$

relating pressure and temperature to enthalpy under supercritical conditions. We have chosen to model this key functional relationship by an exponential polynomial,

$$\begin{aligned} h_{sc}[P,T] \quad &= \beta_0 + \beta_1 P + \beta_2 T + \beta_3 P \exp^{-a(T-T_0)/P} \\ &+ \beta_4 T \exp^{-a(T-T_0)/P} \end{aligned} \tag{4}$$

that we simply fit to the steam table published in [18, pp.89] using standard regression techniques as detailed in the Appendix Section 5.3.1.

This relatively simple (albeit arbitrary) approximation achieves an accuracy of better than 92% (Fig. 21) over the physical range of interest.

As detailed in Appendix Section 5.1.4, we find it necessary to adopt a general PvT relation to get temperature-based dynamics representations for working fluid. Of course, this precludes allowing pressure to play the role of independent variable in the PvT state relations, and we rely on temperature and density as the two independent variables instead. Thus, in equation (3), pressure is actually, in turn, defined by the function

$$P_s = F_H[T_s, \rho_s] \tag{5}$$

derived from empirical studies reported by Haar et al. [11]. Specifically, we achieve 95% accuracy (Fig. 24) by recourse to the quartic approximant

$$F_H[T,\rho] = \rho T(\alpha_0 + \alpha_1\rho + \alpha_2 T + \alpha_3\rho T + \alpha_4 T^2). \tag{6}$$

This model is fit to the tabular data of Haar et al. [11] as described in Appendix Section 5.3.2. Note again, that we have lumped all compressibility effects into the furnace, and fluid flow is assumed not to change through the superheater. Thus appealing to the notion of "mass balance", we treat ρ_s as a constant property in the superheater.

This summarizes the role our various assumptions play in developing the output map formed by composing (1) with (2).

2.3.2 The Internal Dynamics

The dynamics of the internal state — the temperature and density of the furnace; and the temperature of the super heater — is governed by mass balance

$$\frac{d\rho_f}{dt} = \frac{1}{V_f}(w_{fw} - w_{fs}) \tag{7}$$

and heat exchange between the two fluid compartments and the hot wall

$$\begin{aligned}\frac{dT_f}{dt} &= \frac{1}{V_f\eta[P_f,T_f,\rho_f]}(w_{fw}(h_{fec} - h_f) \\ &\quad -(w_{fw} - w_{fs})\tilde{h}[P_f,T_f,\rho_f] + k_{fn}Q_c) \qquad (8)\\ \frac{dT_s}{dt} &= \frac{1}{V_s\eta[P_s,T_s,\rho_s]}(w_{fs}(h_f - h_s) + k_{sh}Q_c) \qquad (9)\end{aligned}$$

Note that in the furnace, again as in the superheater (3), (4), (6), pressure and enthalpy are functions of the independent variables, T_f, ρ_f,

$$\begin{aligned}P_f &= F_H[T_f,\rho_f] \qquad (10)\\ h_f &= h_{sc}[P_f,T_f]. \qquad (11)\end{aligned}$$

V_f and V_s are fluid-tube interior volumes governing mass balance, and k_{fn}, k_{sh}, are heat transfer proportional gains based on the assumption in Section 2.1 and described in Appendix Section 5.1.2.

In contrast, the coefficients governing heat exchange between the compartments are derived by combining the original energy balance equations (42), (43) with (10),(11).

$$\eta[P,T,\rho] = (\rho\frac{\partial h_{sc}}{\partial P}[P,T]-1)\frac{\partial F_H}{\partial T}[T,\rho]+\rho\frac{\partial h_{sc}}{\partial T}[P,T] \quad (12)$$

$$\tilde{h}[P_f,T_f,\rho_f] = (\rho_f\frac{\partial h_{sc}}{\partial P}[P_f,T_f]-1)\frac{\partial F_H}{\partial \rho}[T_f,\rho_f] \quad (13)$$

The only remaining physical phenomena to account for are the coal burning relations,

$$Q_c = \Delta q_c \frac{dM_c}{dt} \quad (14)$$

2.3.3 Abstracted Plant Model

Considering w_{fw},u_v,$\frac{dM_c}{dt}$ as control inputs and W as output, the state space representation of the above model equations may be written more compactly as

$$\frac{d}{dt}\begin{pmatrix}\rho_f\\ T_f\\ T_s\end{pmatrix} = \begin{pmatrix}\frac{1}{V_f} & -\frac{k_v P_s}{V_f\sqrt{T_s}} & 0\\ \frac{h_{fec}-h_f-\tilde{h}}{V_f\eta_f} & \frac{k_v P_s\tilde{h}}{V_f\eta_f\sqrt{T_s}} & \frac{k_{fn}\Delta q_c}{V_f\eta_f}\\ 0 & \frac{k_v P_s(h_f-h_s)}{V_s\eta_s\sqrt{T_s}} & \frac{k_{sh}\Delta q_c}{V_s\eta_s}\end{pmatrix}\begin{pmatrix}w_{fw}\\ u_v\\ \frac{dM_c}{dt}\end{pmatrix} \quad (15)$$

$$W = \frac{k_v P_s(h_s-h_{cd})}{K_{tb}\sqrt{T_s}}u_v \quad (16)$$

2.4 Specific block diagrams

Fig. 2–Fig. 4 are detailed block diagrams with related variables/parameters for the constituent sections of Fig. 1.

The variables shown in these diagrams represent avarage property values in each section, considered as reasonably reflecting the *typical condition* of the section. These property variables are also to be regarded as output values, so enthalpy at outlet of a section is a function of independent properties in the section. The furnace and superheater sections have similar I/O configurations, except that the density in the superheater section is assumed constant due to constant fluid mass flow rate through the section. The throttle valve, where no changes of enthalpy and flow rate exist,

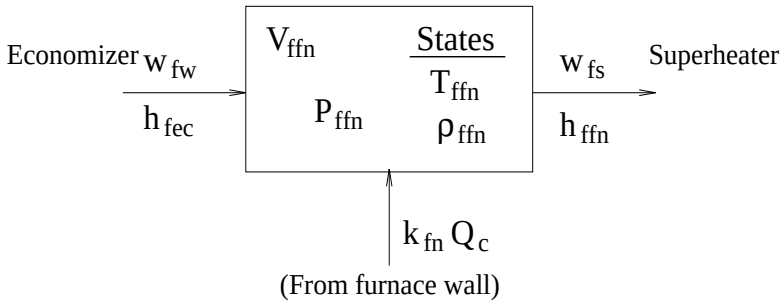

Figure 2: Block diagram of furnace

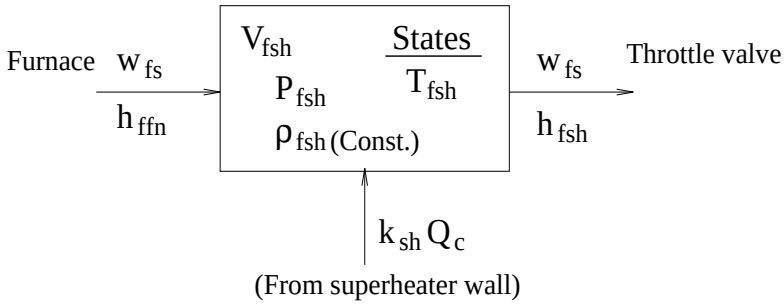

Figure 3: Block diagram of superheater

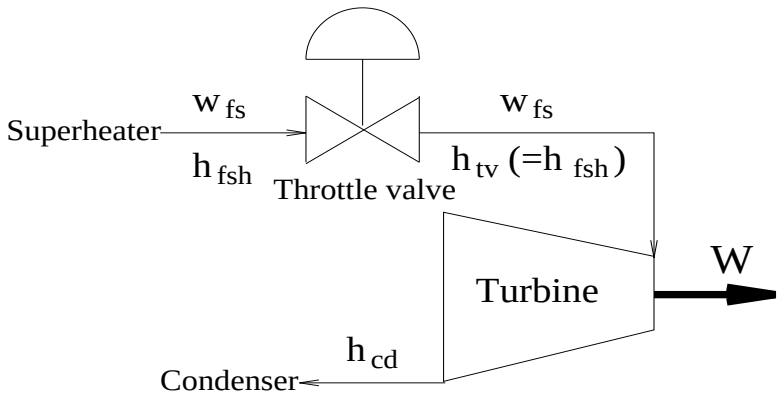

Figure 4: Block diagram of throttle valve and turbine

is controlled directly by its opening value(u_v), affected also by inlet side pressure and temperature, that is, superheater outlet properties. The turbine is characterized by the section enthalpy drop, which is converted into mechanical work by the turbine blades and so generates electric power.

2.5 Control strucure

For purposes of comparison to the EPRI model, a nominal controller was coupled to (15),(16). This modelled controller is, again, extremely simplified relative to the EPRI controller [15]. We limit our attention to load following control, whose main object is to generate the required power designated by supervisory demand controller while maintaining proper conditions on boiler and turbine plants. Fig. 5 shows a block diagram rendering of our simplified version of the load-following controller in the EPRI simulator [15].

In the diagram, $KMW, KULD, KPW, Ktv, Kc$ etc. are normalized constant gains, and some other elements such as nonlinear filters or correction parameters are also approximated to constant values. Load-following control in the EPRI simulator [15] is configured as a turbine following control with feedforward control action, that is, while fuel rate($\frac{dM_c}{dt}$) control functions to make the generated power follow the load demand, throttle valve is controlled to regulate superheater outlet pressure at a designated value(3515psi). In addition, feedwater (demand) is also controlled to regulate load following error[6].

3 Simulation study

3.1 EPRI simulator

The EPRI simulator, a once-through supercritical compact simulator model of a fossil power plant, was developed as part of an EPRI study motivated by the need for effective operator training. Southern California Edison's Ormond Beach Unit 2 is used as the basis for the model, a 750MW gas/oil fired supercritical unit designed for 5.6 million lb/hr flow at 3500 psig and 1000F throttle and 1000F reheat steam condition. The simulator contains feedwater process, boiler, turbines, startup systems, a variety of control loops including load following control, and so on.

[6]In reality, the feedwater pump driven by feedwater pump turbine(s) actually controls the feedwater value. But in our formulation, feedwater demand(w_{fd}) is identified with actual feedwater value(w_{fw}), neglecting its dynamics.

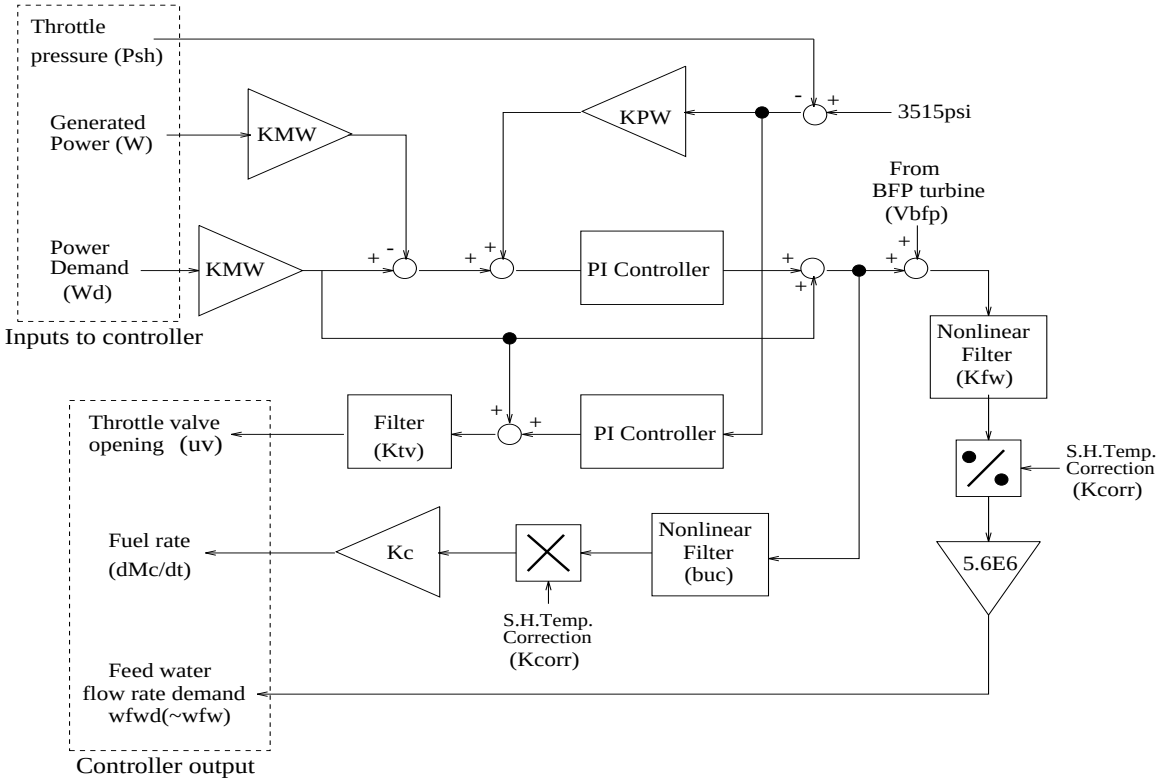

Figure 5: Block diagram of control system

3.2 Some simulation results

We show here some typical simulation results of our model in comparison with the EPRI simulator. Plant and controller models are built in the Mathematica environment and their time responses are calculated using the NDSolve function [19]. The simulations performed here demonstrate load-following control of a trajectory that reduces the generated power from 510MW(steady-state, at t=0) to 450MW at the rate of 5MW/min, considered as a nominal load rate.[7]

Fig. 6 is a load-following control simulation result with our model. The load demand ramp change starts at t=0.1(h), and tracking and regulation behavior is simulated until t=0.6(h). In Fig. 6, solid line and dashed line show the actual power response and the demand respectively. We plot the comparative responses in Fig. 7- 12, where solid lines denote our model and dashed lines denote the EPRI simulator.[8]

The typical I/O responses of our model, such as generated power response, Fig. 7, and control input responses, Fig. 10, Fig. 11, Fig. 12, show favorable fits with EPRI simulator[9]. In contrast, Fig. 8, 9 display large discrepancies in internal state responses. These discrepancies are mainly due to the constant boundary conditions for input enthalpy from economizer in our 'cutout' model as discussed later in the conclusion.

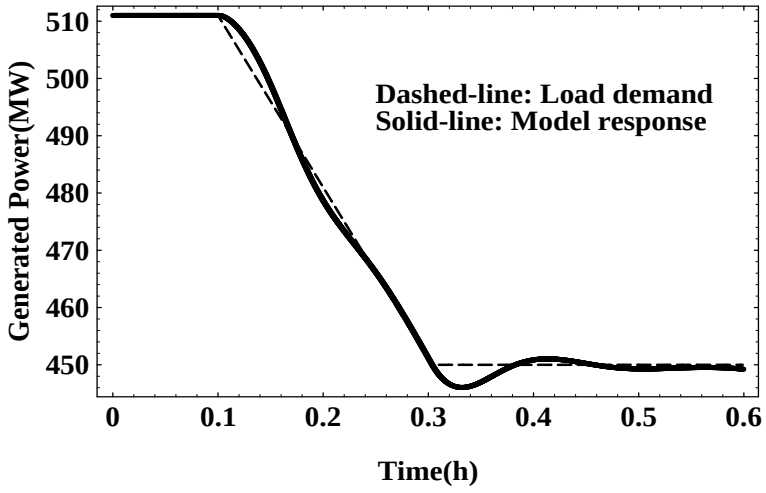

Figure 6: Load following control

[7]The normal load rate is about $0.5\% - 2\%/min.$ for current power generating plants. [9],[15]

[8]The comparison result for the furnace density is omitted because the corresponding data for EPRI simulator is not available

[9]The discrepancy in Fig. 11, between valve opening steady states is due to our omission of a reheater section

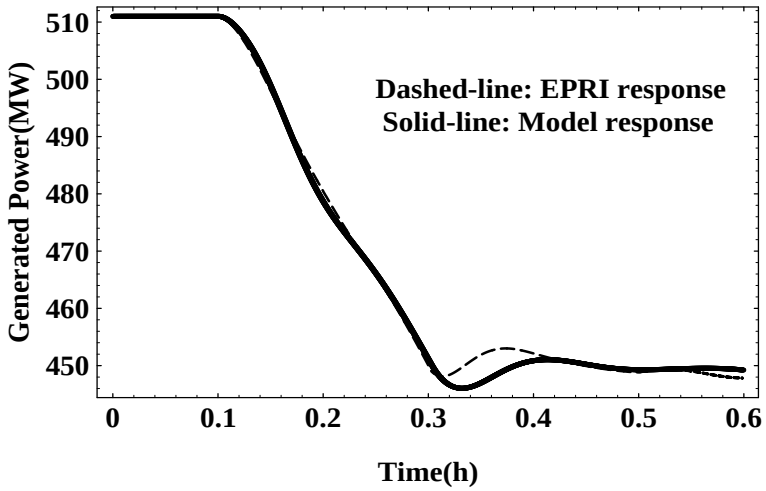

Figure 7: Load following control comparison

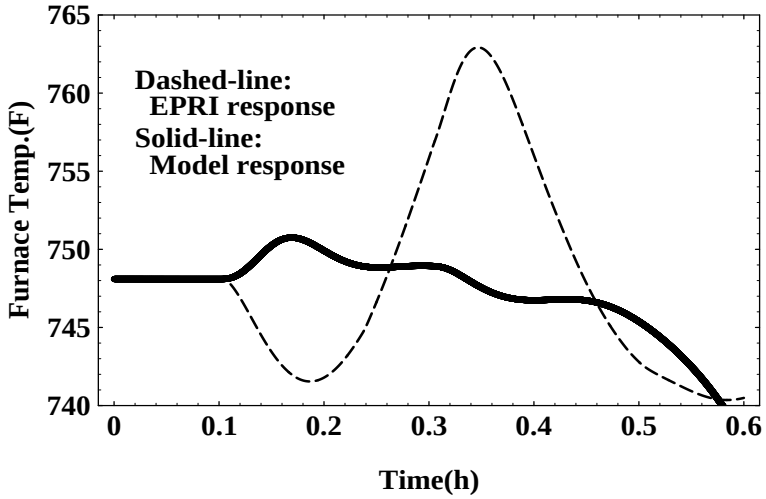

Figure 8: Furnace temperature response comparison

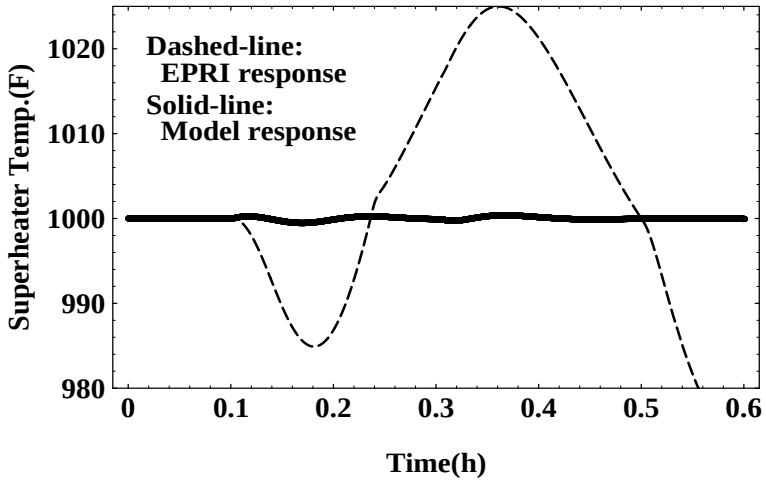

Figure 9: Superheater temperature response comparison

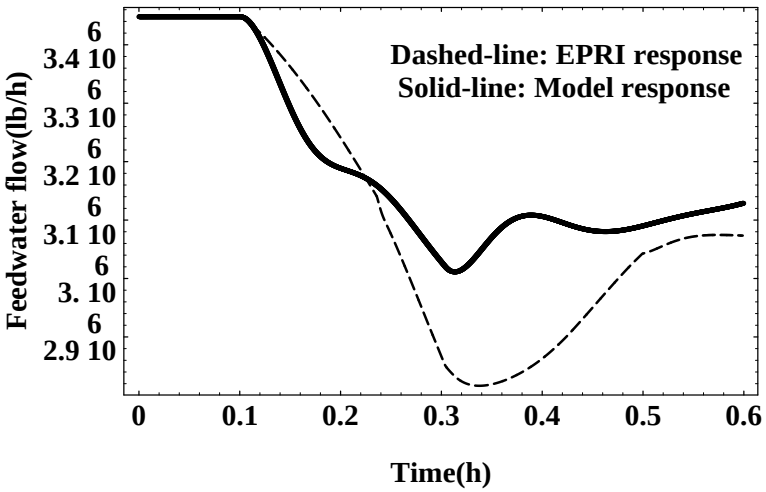

Figure 10: Feedwater flow comparison

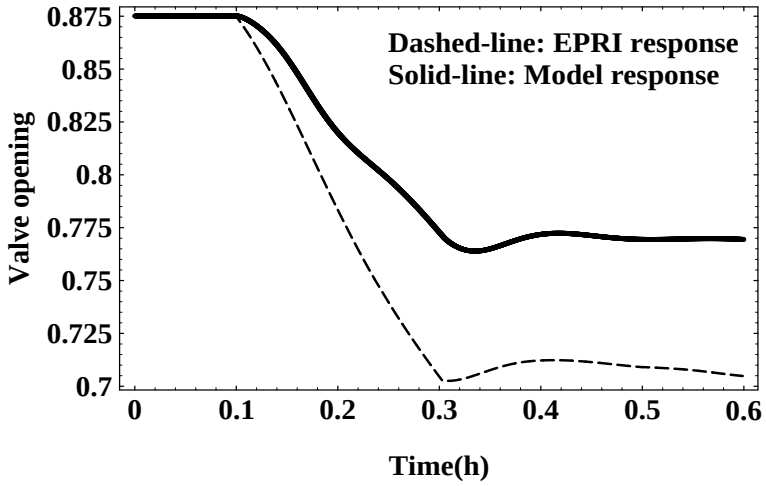

Figure 11: Valve opening comparison

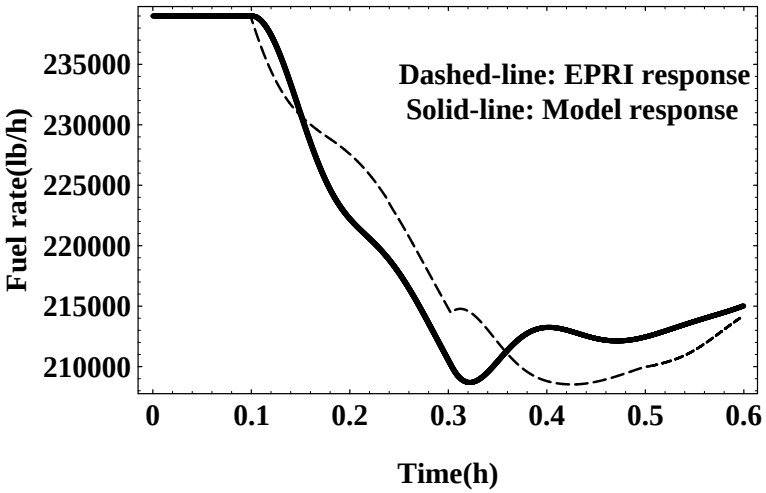

Figure 12: Fuel rate comparison

Our model demonstrates reasonable I/O fit for the operational range roughly from 65% to 90% of the maximum effective load in the EPRI simulator(600MW) [10]. For example, Fig. 13- 18 depict other load following control simulation results in case of changing load demand from 511MW up to 580MW(Fig. 13- 15), and 511MW down to 400MW(Fig. 16- 18). Response fit is poor in the increasing load simulation when demand exceeds the valid range of our model.

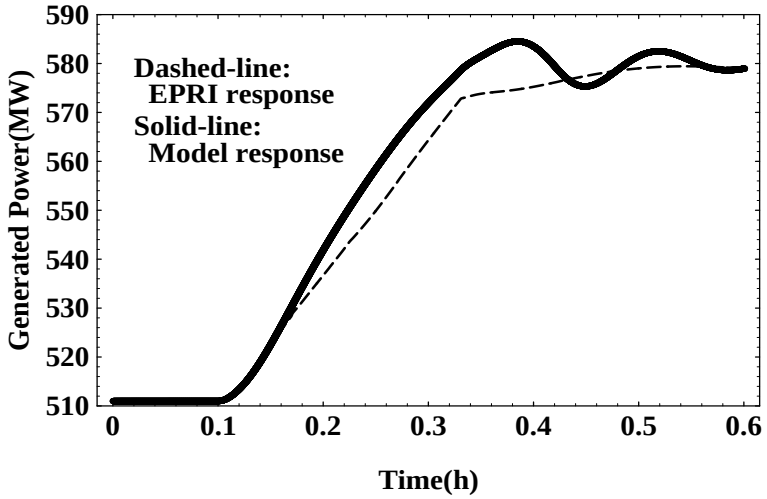

Figure 13: Load following control comparison(511MW→580MW)

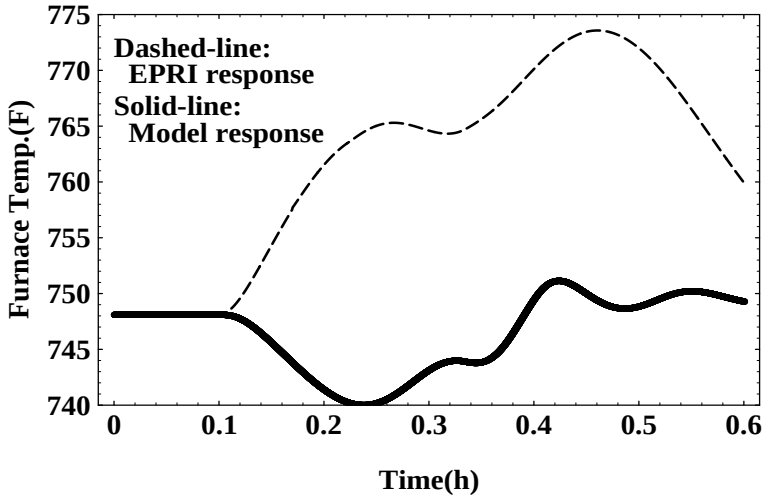

Figure 14: Furnace temp. response comparison(511MW→580MW)

[10]Nominal maximum effective power is claimed as 750MW though, we have been unable to prove the fit beyond this range since the EPRI simulator will not run.

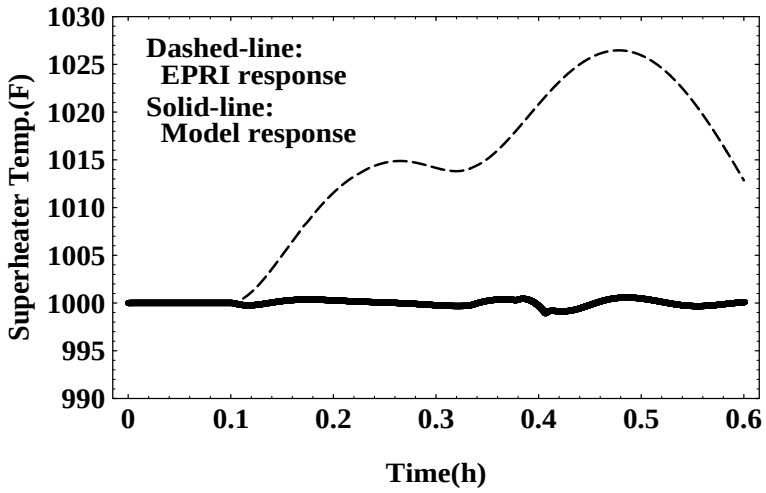

Figure 15: Superheater temp. response comparison(511MW→580MW)

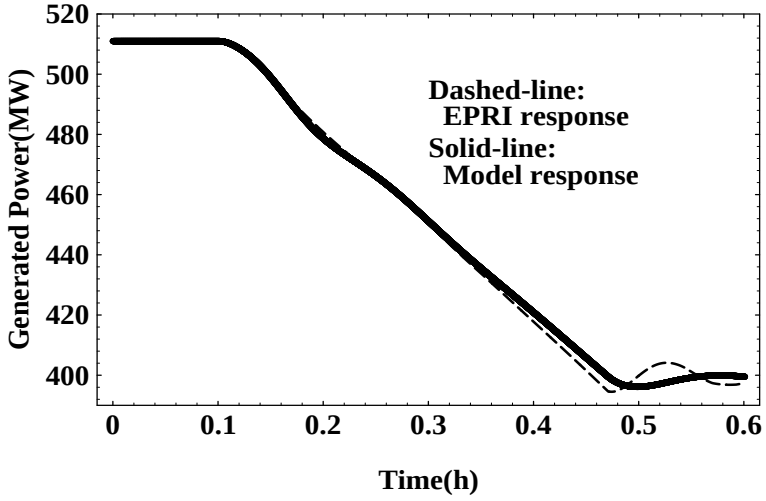

Figure 16: Load following control comparison(511MW→400MW)

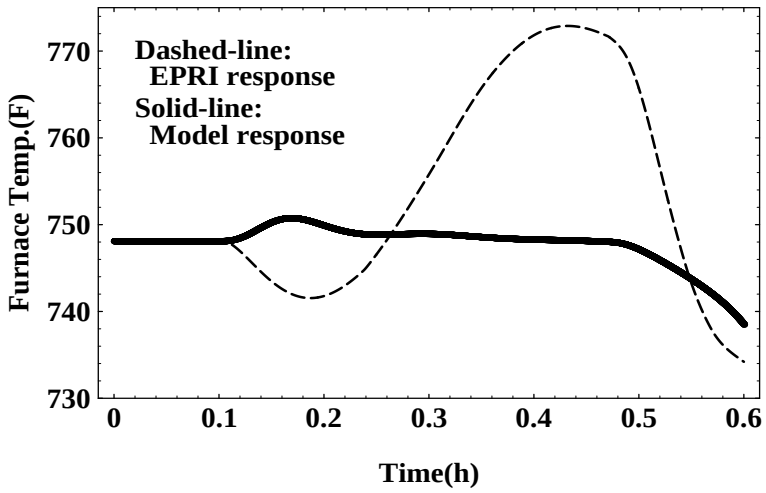

Figure 17: Furnace temp. response comparison(511MW→400MW)

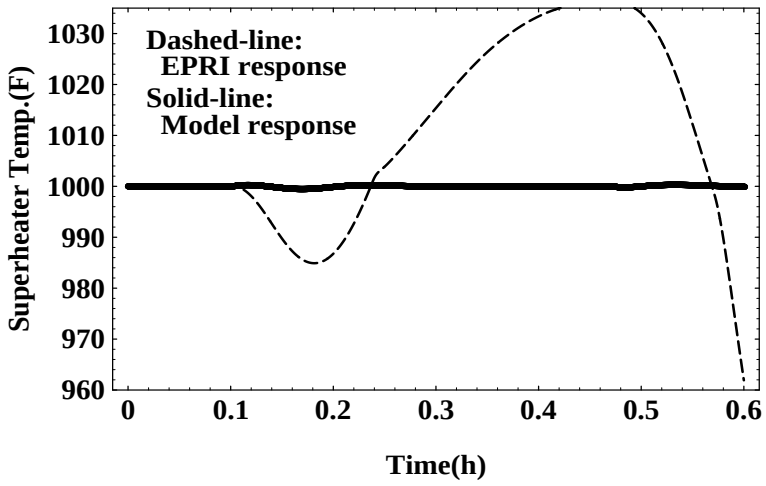

Figure 18: Superheater temp. response comparison(511MW→400MW)

4 Conclusion

We have derived a mathematical model of a supercritical boiler/turbine power plant, emphasizing the simplicity and tractability of the model for the use of intelligent control system design, but still following a physically rooted approach based on laws of mass/energy conservation, supercritical fluid behavior, and so on.

The derived model resuls in a system with 3 control inputs($w_{fw}, u_v, \frac{dM_c}{dt}$), 3 states($\rho_{ffn}, T_{ffn}, T_{sh}$), and 1 output($W$), and has been validated through load-following control simulation. The model seems quite tractable from the viewpoint of nonlinear control, with a state-space form description, $\dot{x} = B(x)u, y = c(x)u$.

We believe the discrepancies between our model and the EPRI simulator, especially observed in the internal state responses, are directly related to the absence of property value estimates: i.e.; the compromise assumptions of constant input enthalpy from economizer(h_{fec}) and the output enthalpy to condenser(h_{cd}). Moreover, due to the elimination of a reheater section, the throttle valve in our model includes the effect of another throttle valve in the reheater outlet, so there exist large differences in valve opening control response.

Adding more sections in the model will enable us to take into account the fluctuations of these properties. At the same time, we will look into the applicability of advanced control designs including some intelligent nonlinear control approaches for this derived model.

5 Appendix

5.1 Physical model derivation

We model here the furnace and the superheater units as blocks composed of one lumped section[11].

In each section, axial heat transfer is assumed negligible and heat transfer from gas to wall and wall to fluid is supposed dominant.

[11] Of course, it would be straightforward to build up a larger model with more sections.

5.1.1 Notation

A complete list of variales which are used for model description follows: [12]

States

Symbol	Parameter	Units
T_{gfn}	Temperature of flue gas in furnace section	F
T_{gsh}	Temperature of flue gas in superheater section	F
ρ_{gfn}	Density of flue gas in furnace section	lb/ft^3
ρ_{gsh}	Density of flue gas in superheater section	lb/ft^3
T_{wfn}	Temperature of wall in furnace section	F
T_{wsh}	Temperature of wall in superheater section	F
ρ_{ffn}	Density of steam in furnace section	lb/ft^3
T_{ffn}	Temperature of steam in furnace section	F
T_{fsh}	Temperature of steam in superheater section	F

Control inputs

Symbol	Parameter	Units
w_{fw}	Input water mass flow rate from economizer section	lb/h
$\frac{dM_c}{dt}$	Combustion rate of coal fuel	lb/h
u_v	Throttle valve opening($0 \leq u_v \leq 1$)	

[12] Being different from the notatin in Section 2.2, we employ here a set of notations applicable for the future model expansion, but a little bit longsome ones. The first character in subscripts of variables indicates a heat transfer medium, that is, 'g' means flue gas, 'w' is wall, and 'f' means working fluid. Also each section name is attached in an abbreviation form like, 'fn'–furnace, 'sh'–superheater, 'ec'– economizer, and so on.

Output

Symbol	Parameter	Units
W	Generated power	MW

Other variables

Symbol	Parameter	Units
w_g	Flue gas mass flow rate	lb/h
h_{gah}	Flue gas enthalpy out of air heater section	Btu/lb
h_{gfn}	Flue gas enthalpy out of furnace section	Btu/lb
h_{gsh}	Flue gas enthalpy out of superheater section	Btu/lb
Q_{gwf}	Heat flow from flue gas to wall in furnace section	Btu/h
Q_{gws}	Heat flow from flue gas to wall in superheater section	Btu/h
Q_c	Combustion heat flow in furnace section	Btu/h
T_{gah}	Temperature of flue gas in air heater section	F
w_{fs}	Steam mass flow rate	lb/h
Q_c	Combustion heat flow in furnace section	Btu/h
P_{ffn}	Pressure of steam in furnace section	psi
P_{fsh}	Pressure of steam in superheater section	psi
h_{fec}	Steam enthalpy in economizer section	Btu/lb
h_{ffn}	Steam enthalpy in furnace section	Btu/lb
h_{fsh}	Steam enthalpy in superheater section	Btu/lb
h_{cd}	Steam enthalpy in condenser section	Btu/lb
ρ_{fsh}	Density of steam in furnace section	lb/ft^3
U_{gws}	Convective heat transfer coefficient	$Btu/h \cdot ft^2 \cdot F$
U_{wff}	Convective heat transfer coefficient under supercritical environment in furnace	$Btu/h \cdot ft^2 \cdot F$
U_{wfs}	Convective heat transfer coefficient under supercritical environment in superheater	$Btu/h \cdot ft^2 \cdot F$

Constants

Symbol	Parameter	Units
C_{vg}	Flue gas constant volume specific heat	$Btu/lb \cdot F$
C_{pg}	Flue gas constant pressure specific heat	$Btu/lb \cdot F$
C_{vw}	Metal constant volume specific heat	$Btu/lb \cdot F$
ε_{gf}	Emittance of flue gas in furnace section	
α_{gf}	Absorptivity of flue gas in furnace section	
σ	Stefan-Boltzman constant	$Btu/h \cdot F^4 \cdot ft^2$
k_{fn}	Gain of heat transfer from gas to wall in the furnace	
k_{sh}	Gain of heat transfer from gas to wall in the superheater	
Δq_c	Calorific value of coal	Btu/lb
k_v	Valve flow rate parameter	$ft \cdot s \cdot F^{1/2}$
K_{tb}	Energy conversion parameter	
ρ_{wfn}	Metal density of wall in furnace section	lb/ft^3
ρ_{wsh}	Metal density of wall in superheater section	lb/ft^3
V_{gfn}	Furnace interior volume	ft^3
V_{gsh}	Superheater interior volume	ft^3
V_{wfn}	Metal volume of furnace wall	ft^3
V_{wsh}	Metal volume of superheater wall	ft^3
V_{ffn}	Fluid tube interior volume in furnace	ft^3
V_{fsh}	Fluid tube interior volume in superheater	ft^3
A_{gwf}	Effective area for gas radiative heat transfer in furnace section	ft^2
A_{gws}	Effective area for gas convective heat transfer in superheater section	ft^2
A_{wff}	Effective area for fluid convective heat transfer in furnace section	ft^2
A_{wfs}	Effective area for fluid convective heat transfer in superheater section	ft^2
A_{cg}	Gas passing cross-sectional area in superheater	ft^2
A_{cff}	Fluid tube cross-sectional area in furnace	ft^2
A_{cfs}	Fluid tube cross-sectional area in superheater	ft^2
d_{ge}	Equivalent diameter of gas passing cross-section	ft
d	Equivalent diameter of fluid passing cross-section	ft
μ_g	Viscosity of flue gas	ft^2/s
μ	Viscosity of fluid(water or steam)	ft^2/s
k_g	Conductivity of flue gas	$Btu/ft \cdot s \cdot R$
k	Conductivity of fluid(water or steam)	$Btu/ft \cdot s \cdot R$

5.1.2 Flue gas

First, we describe the basic relations for flue gas based on the principles of enegy conservation.

Energy balance

$$w_g(h_{gah} - h_{gfn}) - Q_{gwf} + Q_c = V_{gfn}C_{vg}\frac{d(\rho_{gfn}T_{gfn})}{dt} \quad (17)$$

$$w_g(h_{gfn} - h_{gsh}) - Q_{gws} = V_{gsh}C_{vg}\frac{d(\rho_{gsh}T_{gsh})}{dt} \quad (18)$$

where Q_{gwf},Q_{gws},Q_c represent heat transfer from gas to wall in furnace and superheater sections, and by coal combustion respectively. Q_{gwf},Q_{gws} are composed of exclusively radiation heat transfer([2] Chap.4,4-7,8) and convection heat transfer term respectively. They are as follows.

$$Q_{gwf} = A_{gwf}(\varepsilon_{gf}\sigma T_{gfn}^4 - \alpha_{gf}\sigma T_{wfn}^4) \quad (19)$$

$$Q_{gws} = U_{gws}A_{gws}(T_{gsh} - T_{wsh}) \quad (20)$$

$$Q_c = \Delta q_c\frac{dM_c}{dt} \quad (21)$$

According to [2](Chap.4,4-13), heat transfer coefficient(U_{gws}) between gas and wall in superheater section is given experimentally,

$$U_{gws} = 0.023(\frac{(\frac{w_g}{A_{cg}})^{0.8}}{d_{ge}^{0.2}})(\frac{C_{pg}^{0.4}k_g^{0.6}}{\mu_g^{0.4}})(\frac{T_{gsh}}{\frac{T_{gsh}+T_{wsh}}{2}})^{0.8} \quad (22)$$

As described in Section 2.1, we assume for gas behavior,

- Flue gas is ideal $\Rightarrow \rho_g T_g = \frac{P_g}{R_g}$
- Momentum of fluid gas is negligible $\Rightarrow P_g = const.$

Thus, the right hand side in equations (17), (18) vanish, and energy balance equations are rewritten as

$$w_g(h_{gah} - h_{gfn}) - Q_{gwf} + Q_c = 0 \quad (23)$$

$$w_g(h_{gfn} - h_{gsh}) - Q_{gws} = 0 \quad (24)$$

Because $P_g = const.$, each enthalpy drop is approximated as follows,

$$h_{gah} - h_{gfn} = C_{pg}(T_{gah} - T_{gfn}) \quad (25)$$
$$h_{gfn} - h_{gsh} = C_{pg}(T_{gfn} - T_{gsh}), \quad (26)$$

resulting in the following nonlinear algebraic equations,

$$w_g C_{pg}(T_{gah} - T_{gfn}) - Q_{gwf}[T_{gfn}, T_{wfn}] + Q_c[\dot{M}_c] = 0 \quad (27)$$
$$w_g C_{pg}(T_{gfn} - T_{gsh}) - Q_{gws}[T_{gsh}, T_{wsh}] = 0, \quad (28)$$

that represent the steady-state relations. The first term of Eq. 27 represents an increase amount of heat conveyed by flue gas through the furnace section, and the second term(Q_{gwf}) is a heat transfer from flue gas to wall. These two heat flow could be considered to result from the combustion heat(Q_c). By summing two Eqs. 27 and 28, the same interpretation holds for a heat increase of fluid through the furnace and superheater, and Q_{gws}. The assumption newly introduced by us in Section 2.1 for working around a direct solution of Eqs. 27 and 28, maintains that these heat transfer from fluid to wall are proportional to the combustion heat as follows.

$$Q_{gwf} = k_{fn} Q_c \quad (29)$$
$$Q_{gws} = k_{sh} Q_c \quad (30)$$

From the above observations, this assumption means the ratios, by which the combustion heat is used for fluid heat increase and heat transfer to the wall, is kept constant through operations.

5.1.3 Wall

Dynamic relations for walls are also based on their combined heat transfer exchanges between flue gas and wall, and wall and fluid, written down as follows. As in the case of flue gas, heat transfer in the axial direction is negligible, and energy conservation again yields.

Energy balance

$$Q_{gwf} - Q_{wff} = V_{wfn} \rho_{wfn} C_{vw} \frac{dT_{wfn}}{dt} \quad (31)$$
$$Q_{gws} - Q_{wfs} = V_{wsh} \rho_{wsh} C_{vw} \frac{dT_{wsh}}{dt} \quad (32)$$

In contrast to the gas-wall exchange, heat transfer from wall to fluid is exclusively convective

$$
\begin{aligned}
Q_{wff} &= U_{wff} A_{wff} (T_{wfn} - T_{ffn}) && (33)\\
Q_{wfs} &= U_{wfs} A_{wfs} (T_{wsh} - T_{fsh}). && (34)
\end{aligned}
$$

In these equations, heat transfer coefficients under supercritical condition are defined as follows([14]).

$$
\begin{aligned}
U_{wff} &= 0.00459 (\frac{k}{d}) (\frac{dw_{fw}}{\mu A_{cff}})^{0.923} (\frac{h[P_{ffn}, T_{wfn}] - h[P_{ffn}, T_{ffn}]}{T_{wfn} - T_{ffn}} \frac{\mu}{k})^{0.613} \\
&\quad (\frac{\rho[P_{ffn}, T_{wfn}]}{\rho_{ffn}})^{0.231} && (35)\\
U_{wfs} &= 0.00459 (\frac{k}{d}) (\frac{dw_{fs}}{\mu A_{cfs}})^{0.923} (\frac{h[P_{fsh}, T_{wsh}] - h[P_{fsh}, T_{fsh}]}{T_{wsh} - T_{fsh}} \frac{\mu}{k})^{0.613} \\
&\quad (\frac{\rho[P_{fsh}, T_{wsh}]}{\rho_{fsh}})^{0.231} && (36)
\end{aligned}
$$

Thus, the dynamics for T_{wfn} and T_{wsh} might be written

$$
\begin{aligned}
\frac{dT_{wfn}}{dt} &= \frac{1}{V_{wfn} \rho_{wfn} C_{vw}} (Q_{gwf} - Q_{wff}) && (37)\\
\frac{dT_{wsh}}{dt} &= \frac{1}{V_{wsh} \rho_{wsh} C_{vw}} (Q_{gws} - Q_{wfs}) && (38)
\end{aligned}
$$

but, in keeping with the assumption laid out above, we assume that the gas-wall exchange is far faster than the wall-steam exchange, and take the heat transfer through wall to be always balanced,

$$
\begin{aligned}
Q_{gwf} &= Q_{wff} && (39)\\
Q_{gws} &= Q_{wfs}. && (40)
\end{aligned}
$$

5.1.4 Working fluid

In the past works, pressure for working fluid(water,steam), has been evaluated by its stationary relation called "pressure drop"[13]([5], [9]) But we'd

[13]Under stationary conditions, a relation, $P_{in} - Pout = \kappa \frac{w}{\rho}$ holds for inlet-outlet pressures. This relation gives us a simple method for estimating pressure in each section, but not useful for evaluating its derivative.

like to derive a fluid dynamics of temperature-as-state, not of internal energy formulated in the past developments([5], [9]), we need to adopt a general PvT equation to evaluate a derivative of pressure by a derivative of temperature (and density). A general PvT equation proposed by Haar et.al. [11] was actually adopted to this end.

Mass balance - Furnace sections -

Compressibility effect is lumped into furnace section, that is, there exists the difference between inlet and outlet fluid mass flow rate (w_{fw}, w_{fs}) not in steady state.

$$\frac{d\rho_{ffn}}{dt} = \frac{1}{V_{ffn}}(w_{fw} - w_{fs}) \tag{41}$$

Energy balance

$$w_{fw}h_{fec} - w_{fs}h_{ffn} + Q_{wff} = V_{ffn}\frac{d(\rho_{ffn}u_{ffn})}{dt} \tag{42}$$

$$w_{fs}(h_{ffn} - h_{fsh}) + Q_{wfs} = V_{fsh}\rho_{fsh}\frac{du_{fsh}}{dt} \tag{43}$$

From the definition of enthalpy($h = u + P/\rho$), property table approximation for enthalpy in supercritical region($P > 3208psi, T > 705F$)(Eq. 44 and general PvT equation(45)(Ref. [11]), we can rewrite (42)-(43) as (46)-(47), taking into account density dynamics in the furnace.

$$h = h_{sc}[P, T] \tag{44}$$

$$P = F_H[T, \rho] \tag{45}$$

$$\frac{dT_{ffn}}{dt} = \frac{1}{V_{ffn}\eta[P_{ffn}, T_{ffn}, \rho_{ffn}]}(w_{fw}(h_{fec} - h_{ffn}) - (w_{fw} - w_{fs})\tilde{h}[P_{ffn}, T_{ffn}, \rho_{ffn}] + Q_{wff}) \tag{46}$$

$$\frac{dT_{fsh}}{dt} = \frac{1}{V_{fsh}\eta[P_{fsh}, T_{fsh}, \rho_{fsh}]}(w_{fs}(h_{ffn} - h_{fsh}) + Q_{wfs}) \tag{47}$$

where $\eta, \tilde{h}$ denote nonlinear state-dependent coefficients described in detail as follows.

$$\eta[P,T,\rho] = (\rho\frac{\partial h_{SC}}{\partial P}[P,T]-1)\frac{\partial F_H}{\partial T}[T,\rho] + \rho\frac{\partial h_{SC}}{\partial T}[P,T] \quad (48)$$

$$\tilde{h}[P_{ffn},T_{ffn},\rho_{ffn}] = (\rho_{ffn}\frac{\partial h_{SC}}{\partial P}[P_{ffn},T_{ffn}]-1)\frac{\partial F_H}{\partial \rho}[T_{ffn},\rho_{ffn}] \quad (49)$$

Now, combining Eq. 29, 30, 39, 40, 46, and 47, we get the final dynamics representation for fluid temperatures,

$$\frac{dT_{ffn}}{dt} = \frac{1}{V_{ffn}\eta[P_{ffn},T_{ffn},\rho_{ffn}]}(w_{fw}(h_{fec}-h_{ffn})-(w_{fw}-w_{fs})\tilde{h}[P_{ffn},T_{ffn},\rho_{ffn}] + k_{fn}Q_c) \quad (50)$$

$$\frac{dT_{fsh}}{dt} = \frac{1}{V_{fsh}\eta[P_{fsh},T_{fsh},\rho_{fsh}]}(w_{fs}(h_{ffn}-h_{fsh})+k_{sh}Q_c) \quad (51)$$

5.2 Model in turbine section

5.2.1 Throttle valve

Generated power is directly and instantly adjusted by throttle valve control, resulting in steam flow control through turbine. Steam flow rate through valve is reasonably considered as a function of valve opening, inlet flow pressure(superheater outlet flow pressure) and inlet flow temperature(superheater outlet flow temperature), modelled as follows(Ref. [9] and [10])[14].

Throttle valve flow

$$w_{fs} = \frac{k_v P_{fsh}}{\sqrt{T_{fsh}}}u_v \quad (52)$$

where u_v represents valve opening, taking a value in [0,1]. Further, enthalpy drop through valve is assumed to be negligible.

[14]Eq. 52 can be derived based on the assumption of the ideal gas behavior for steam through valve. Although we could adopt more accurate representation, $w_{fs} = k_v\sqrt{P_{fsh}\rho_{fsh}}u_v$, its use forces us to build a nonlinear approximation fitting of density(ρ_{fsh}) as $\rho_{fsh} = \rho_{sc}[P_{fsh},T_{fsh}]$. We employ here the simpler form considering its reasonable applicability even for supercritical range.

$$h_{fsh} = h_{tv} \tag{53}$$

5.2.2 Turbine

As mentioned above, power generated by turbine is approximately proportional to both of steam flow rate through turbine and its enthalpy drop. Assuming negligible loss of heat dissipation and steam extraction in turbine, we employed the following relation for evaluating its generated power.

$$w_{fs}(h_{tv} - h_{cd}) = K_{tb}W \tag{54}$$

where h_{cd} is an enthalpy of a condenser, regarded as constant.

5.3 Constitutive property approximation

In this section, some approximation results for constitutive functions used in our model are shown.

5.3.1 Enthalpy approximation in supercritical region

As with other properties, enthalpy of steam changes drastically around critical point. Fig. 19 shows its behavior in the range of supercritical region($3000psi < P < 4000psi, 700F < T < 1100F$).

We approximated this enthalpy property using some intuitively derived exponential-like functions represented in Eq. 4. In approximate equation, paremeters included nonlinearly, such as, a, T_0 are fixed through trial-and-error rough fitting evalutions, after that, a standard regressin technique is applied for estimating proper values of parameters linearly included. Approximated enthalpy function and its relative error to original one are shown in the followin Fig. 20- 21.

5.3.2 Approximation of Haar function

Original general reference function proposed by Haar [11] is shown graphically in Fig. 22. This haar function is approximated by a quartic function(Eq. 6), whose parameters also estimated using the same standard regression method as with the enthalpy approximation. The approximation results, including relative error of appriximation, are shown in Fig. 23- 24.

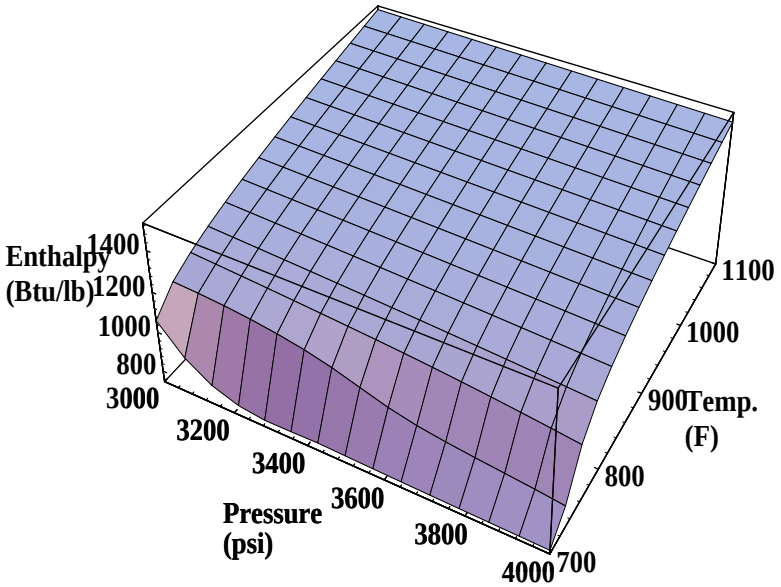

Figure 19: Enthalpy in supercritical region

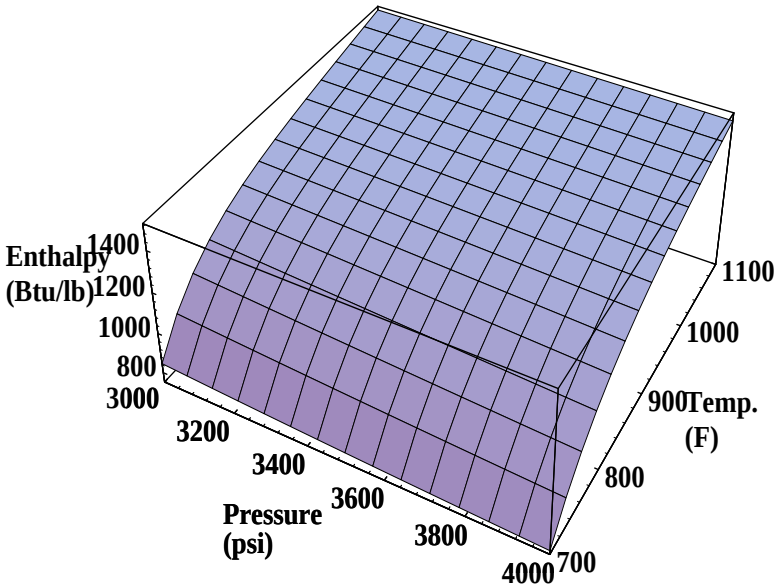

Figure 20: Approximated enthalpy function

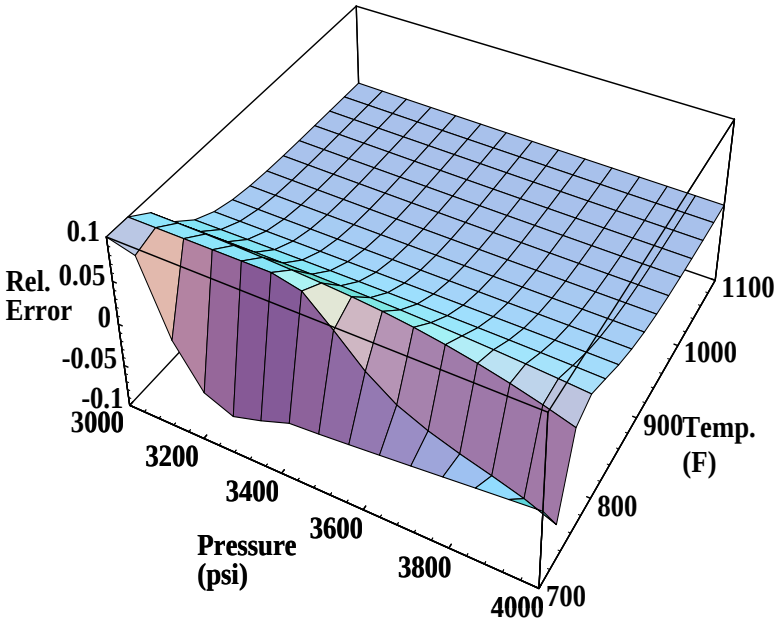

Figure 21: Relative error for enthalpy approximation

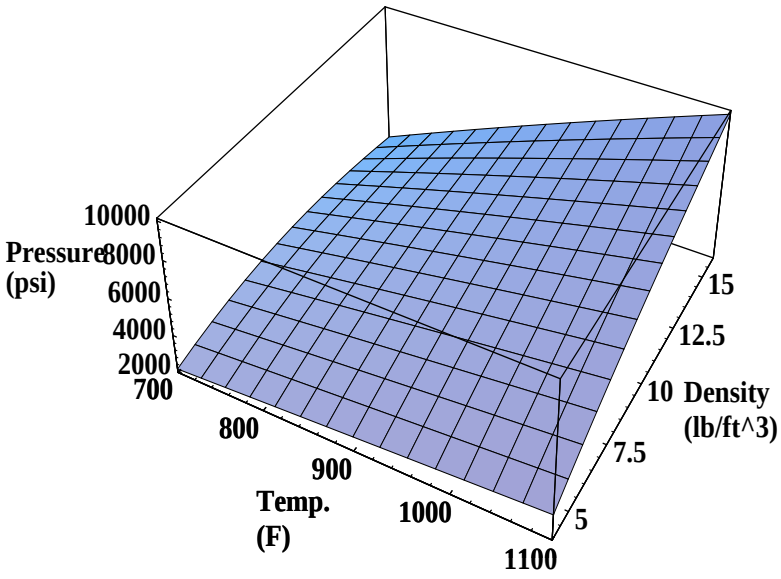

Figure 22: General reference function by Haar

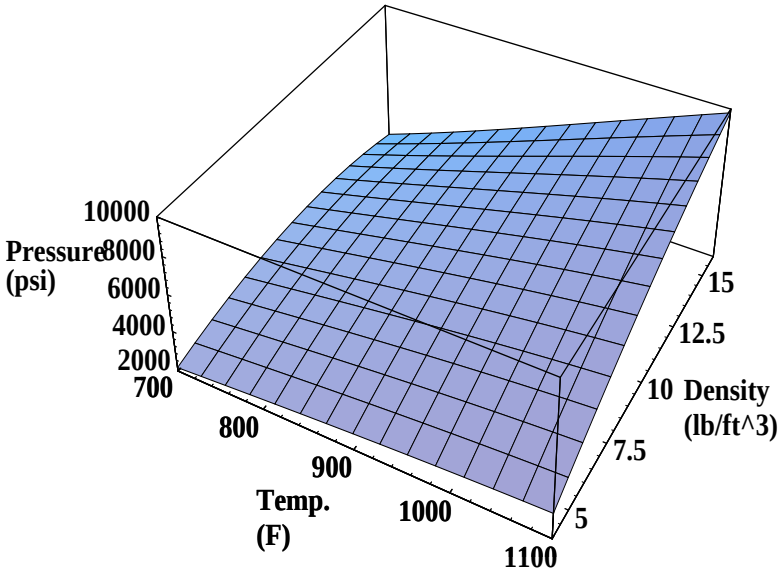

Figure 23: Approximated haar function

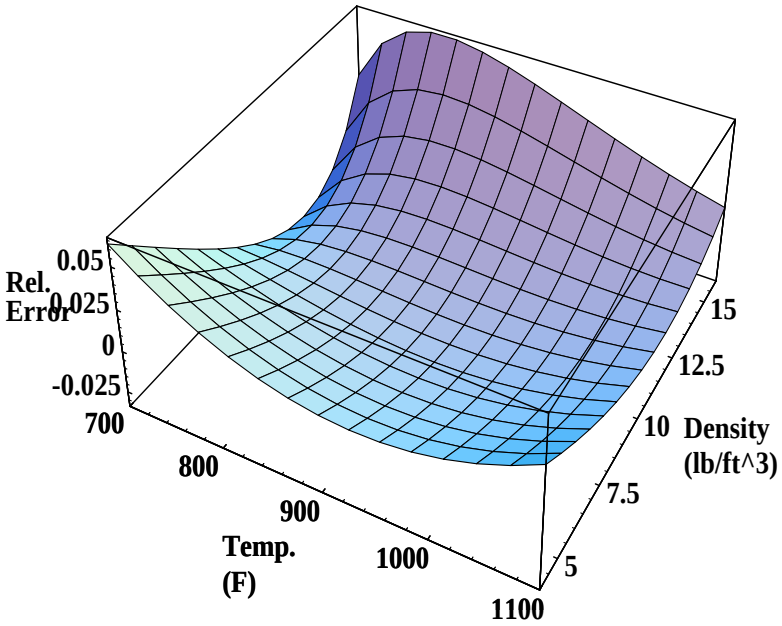

Figure 24: Relative error for Haar function approximation

5.4 Model parameter calibration

To make our model consistent with the EPRI model for simulating plant response, some crucial model parameters were calibrated using an initial condition of '511MW-steady state' in EPRI simulator.

Specifically, in Eq.(7), (8), (9), and (16), the right-hand-side was evaluated at the steady-state EPRI state values($\rho_f = {\rho_f}^*, T_f = {T_f}^*, T_s = {T_s}^*$), and control values($w_{fw} = w^*_{fw}, u_v = u^*_v, \frac{dM_c}{dt} = \frac{dM_c}{dt}^*$). Then, the parameters, k_v, k_{fn}, k_{sh},and K_{tb} were calculated so as to solve the following steady state equations.

$$0 = {w_{fw}}^* - \frac{k_v {P_s}^*}{\sqrt{{T_s}^*}} {u_v}^* \tag{55}$$

$$0 = {w_{fw}}^*(h_{fec} - h_f) - ({w_{fw}}^* - \frac{k_v {P_s}^*}{\sqrt{{T_s}^*}} {u_v}^*)\tilde{h} + k_{fn} Q_c(\frac{d{M_c}^*}{dt}) \tag{56}$$

$$0 = \frac{k_v {P_s}^*}{\sqrt{{T_s}^*}} {u_v}^*(h_f - h_s) + k_{sh} Q_c(\frac{d{M_c}^*}{dt}) \tag{57}$$

$$W^*(= 511MW) = \frac{k_v {P_s}^*}{\sqrt{{T_s}^*}} {u_v}^* \frac{h_s - h_{cd}}{K_{tb}} \tag{58}$$

References

[1] C.Maffezzoni, Concepts practice and trends in fossil-fired power plant control, *IFAC Power Systems and Power Plant Control*, pp.1-9, Beijing, 1986

[2] S.C.Stultz and J.B.Kitto editors, Steam: It's Generation and Use, Babcock and Wilcox,Inc., Barberton, Ohio, 40-th edition, 1992.

[3] P.Profos, Supercritical Pressure and Efficiency of Steam Power Plants, *Sulzer Technical Review* 4, pp.11-18, 1958

[4] K.J. Åström and K.Eklund, A Simplified Non-Linear Model of a Drum Boiler-Turbine Unit, *Int.J.Control*, Vol.16, No.1, pp.145-169, 1972

[5] J.Adams,D.R.Clark,J.R.Louis and J.P.Spanbauer, Mathematical model of once-through boiler dynamics, *IEEE Transactions on Power Systems*, Vol.84, pp.146-156, February 1965.

[6] A.Ray and H.F.Bowman, A nonlinear dynamic model of a once-through subcritical steam generator, *Journal of Dynamic Systems, Measurement and Control*, Vol.98, pp.1-8, September 1976.

[7] G.Y.Masada and D.N.Wormly, Dynamic Model of a 1400 MW Supercritical Pressure Steam Plant, ASME paper, 82-JPGC-Pwr-13, pp.1-9, 1982.

[8] G.Y.Masa and D.N.Wormley, Evaluation of lumped parameter heat exchanger dynamic models, ASME paper, 82-WA/DSC-16, pp.1-10.

[9] G.Y.Masada, Modeling and Control of Power Plant Boiler-Turbine-Generator Systems, Sc.D.Thesis,MIT,Dept.of Mechanical Engineering, Nov. 1979.

[10] J.K.Salisbury, Steam Turbines and their Cycles, John Wiley and Sons,Inc.,1950.

[11] L.Haar et.al, Thermodynamic properties for fluid water, in *J. Straub and K. Scheffler (eds.) Pergamon Press 1980*, pp.69-82.

[12] D.Gunn and R.Horton, Industrial Boilers, Longman Scientific & Technical, 1989.

[13] W.L.Haberman and J.E.John, Engineering Thermodynamics with Heat Transfer, Allyn and Bacon, Massachusetts, 1989.

[14] H.S.Swenson, J.R.Carver, and C.R.Kakarala, Heat Transfer to Supercritical Water in Smooth-Bore Tubes, *Journal of Heat Transfer*, Vol.87, pp.477-484, 1965.

[15] Compact Simulator Manual -Ormond Beach Unit2 Supercritical boiler/turbine-, Electric Power Research Institute and TRAX Corporation, 1993.

[16] R.Shoureshi and H.M.Paynter, Simple Model for Dynamics and Control of Heat Exchangers, *Conference name not available* FP7- 2:30

[17] L.Borsi, Extended Linear Mathematical Model for a Power Station Unit with a Once-Through Boiler, Siemens Forsch.-u.Entwickl. -Ber.Bd. 3 (1974) Nr.5 by Springer-Verlag, pp.274-280, 1974.

[18] 1967 Steam Tables, St.Martine's Press, NewYork, 1967

[19] Wolfram and Stephen, Mathematica: A System for Doing Mathematics by Computer, Addison-Wesley, 1991

[20] Personal communication. Mr.Don Frerichs, Bailey Controls,Inc.